Cancer Immunol Immunother
DOI 10.1007/s00262-007-0387-z

ORIGINAL ARTICLE

Improving alloreactive CTL immunotherapy for malignant gliomas using a simulation model of their interactive dynamics

Natalie Kronik · Yuri Kogan · Vladimir Vainstein · Zvia Agur

Received: 2 May 2007 / Accepted: 7 August 2007

Abstract Glioblastoma (GBM), a highly aggressive (WHO grade IV) primary brain tumor, is refractory to traditional treatments, such as surgery, radiation or chemotherapy. This study aims at aiding in the design of more efficacious GBM therapies. We constructed a mathematical model for glioma and the immune system interactions, that may ensue upon direct intra-tumoral administration of ex vivo activated alloreactive cytotoxic-T-lymphocytes (aCTL). Our model encompasses considerations of the interactive dynamics of aCTL, tumor cells, major histocompatibility complex (MHC) class I and MHC class II molecules, as well as cytokines, such as TGF-β and IFN-γ, which dampen or increase the pro-inflammatory environment, respectively. Computer simulations were used for model verification and for retrieving putative treatment scenarios. The mathematical model successfully retrieved clinical trial results of efficacious aCTL immunotherapy for recurrent anaplastic oligodendroglioma and anaplastic astrocytoma (WHO grade III). It predicted that cellular adoptive immunotherapy failed in GBM because the administered dose was 20-fold lower than required for therapeutic efficacy. Model analysis suggests that GBM may be eradicated by new dose-intensive strategies, e.g., 3×10^8 aCTL every 4 days for small tumor burden, or 2×10^9 aCTL, infused every 5 days for larger tumor burden. Further analysis pinpoints crucial bio-markers relating to tumor growth rate, tumor size, and tumor sensitivity to the immune system, whose estimation enables regimen personalization. We propose that adoptive cellular immunotherapy was prematurely abandoned. It may prove efficacious for GBM, if dose intensity is augmented, as prescribed by the mathematical model. Re-initiation of clinical trials, using calculated individualized regimens for grade III–IV malignant glioma, is suggested.

Keywords Mathematical model · Glioblastoma (GBM) · Adoptive immunotherapy · TGF-β · Interferon-γ

N. Kronik · Y. Kogan · V. Vainstein · Z. Agur (✉)
Institute for Medical BioMathematics (IMBM), 10 Hate'ena St., P.O. Box 282, Bene Ataroth 60991, Israel
e-mail: agur@imbm.org

N. Kronik
e-mail: natalie@imbm.org

Introduction

Adult primary malignant gliomas (MG) are among the most deadly forms of cancer. Median survival for high grade MG varies from 1 year for GBM (Grade IV) to 3 to 5 years for grade III MG [21, 22]. Due to their genomic instability, heterogeneity, and infiltrative behavior in their sequestered location beyond the blood brain barrier (BBB), MG are refractory to conventional treatments, including surgery, radiation, and chemotherapy. Thus, novel therapies are sought, notably immunotherapy, in the hope they offer a survival advantage.

Systemic immunotherapy by vaccination [38], exogenous administration of immune cells or immunoregulatory factors, has been tested as a treatment for many types of cancer, so far with limited success [27, 28, 30, 43, 46]. A different approach was employed by Kruse et al. [24] and Kruse and Rubinstein [25], who report six patients treated by aCTL, three of whom were recurrent grade III MG patients (anaplastic astrocytoma and anaplastic oligodendroglioma) and the other three were recurrent GBM patients. All six patients underwent tumour debulking operations prior to the start of the adjuvant immunotherapy. The six patients were treated with periodic intra-tumoral

aCTL infusions given with a subgleal Rickham reservoir/catheter system 2–3 times within 2 weeks, followed by a rest period of 6 weeks. This process could be repeated up to five times. The total doses of administered aCTL varied between 10^8 and 5.2×10^9 cells [25].

Although technically more complicated, passive aCTL immunotherapy overcomes two major problems encountered with systemic immunotherapy: (1) it is independent of the patient's own often anergic immune system, and (2) the use of intracranial infusion bypasses the BBB. Indeed, the above clinical trial showed success in that two of the grade III patients survived for at least 12 years after treatment [Prof. Carol Kruse (Sidney Kimmel Cancer Center), personal communication] and one survived for 40 months post-treatment. However, all GBM patients died within several months. This discrepancy between the success in curing grade III MG and the failure of GBM immunotherapy points to a crucial difference between the characteristic system dynamics in the two indications. This difference may be clarified by analyzing the reaction rates governing the two processes.

The dynamics of tumor-immune system interactions are complex, involving cytotoxic processes, cytokine modulation and extra-cellular matrix proteins implicated in tumor and immune cell migration, as well as negative and positive feedbacks by paracrine and autocrine factors. Tumor cells use different ways to evade the immune attack. One of them is a dramatic reduction in the expression of major histocompatibility complex (MHC) molecules on their surface [35, 48], which weakens their detection by cytotoxic T-lymphocytes ($CD8^+$). Tumor-produced factors, such as TGF-β, prostaglandin E and interleukin (IL)-10 can suppress helper T lymphocytes ($CD4^+$), as well as stimulate and mobilize regulatory T cells (Tregs). TGF-β is especially important in immunotherapy resistance, particularly with regard to aCTL treatment resistance [9, 12, 13, 44], and also shows negative correlation with response to immunotherapy by dendritic cells [27].

In the central nervous system (CNS), cancer–immune system cellular interactions are influenced by the presence of the selective BBB. Only activated T lymphocytes gain entry to the brain [17]. Lymphocytes infiltrating the brain may lose activated status or may be largely of the immunosuppressive Treg type [2, 18, 34, 39]. Furthermore, the cytokine, TGF-β, whose levels are naturally high in the CNS can influence their function [17]. TGF-β suppresses the production of both IL-1 and MHC class II by antigen-presenting cells (APCs), and also suppresses the activation and proliferation of CTLs [40, 42]. This down-regulation can be balanced by other cytokines, such as IFN-γ, which can increase expression of MHC class I and class II molecules on the surface of tumor cells and microglia [8, 31, 37, 47]. In addition, IFN-γ increases T cell migration across the BBB [17]. To study the delicate balance between activation of the immune response to the tumor and its suppression, a quantitative description of these dynamics is required.

Although the latter seems a daunting task, over the past 30 years complex biological dynamics involved in cancer growth and therapeutics have been studied successfully by mathematical modelling. Consequently, improved chemotherapy and supportive treatment methods have been put forward [1, 3, 11, 36]. In particular, theoretical models of cancer immunology and immunotherapy have been suggested, describing an innate CTL response to the growth of an immunogenic tumor [20, 26] and predicting the efficacy of adoptive immunotherapy [4]. Other models describe immunotherapy using autologous natural killer cells and $CD8^+$ cells [32], or include the effects of chemotherapy and vaccination [33]. Recently, a mathematical model for immunotherapy by IL-21 was suggested and retrospectively validated by experimental results in cancer-bearing animals [7].

In this work we construct a mathematical model for MG adoptive immunotherapy, which describes the complex interactions of tumor cells with aCTL and MHC receptors, mediated by TGF-β and IFN-γ. We supply the model with parameters we have evaluated from in vitro and in vivo results in animals and in humans. The complete model is then used to retrieve various immunotherapeutic scenarios and its predictions are validated by their comparison with two sets of empirical results, those of Burger et al. [6] and those of Kruse et al. [24] and Kruse and Rubinstein [25]. We then complement the study by simulations for identifying improved immunotherapy schedules and for indicating where intervention can lead to a cure.

Methods

Mathematical model

A mathematical model is aimed at yielding a simplified description of the biological process. By singling out the crucial forces in the system and deliberately disregarding secondary effects, the analytical power of the model is significantly sharpened. Our model (Fig. 1) focuses on the main interactions between MG grade III or GBM tumor cells and the host's immune system; brain and peripheral blood are considered as two compartments that are separated by the BBB. The mathematical model, describing treatment with aCTL, takes into account two immune cell sources: adoptive transfer of ex vivo activated lymphocytes placed intracranially in passive immunotherapy and endogenously activated lymphocytes in cell-mediated response. Total number of CTL in the system will be

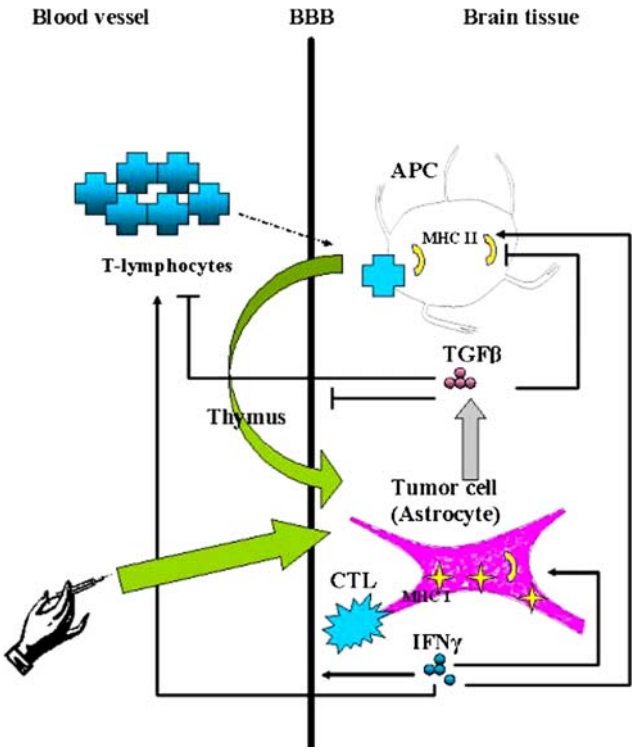

Fig. 1 MG-immune cell interactions. For a long term effective active immune response endogenous $CD4^+$ T lymphocytes (*cross*) may have to cross the BBB (*black bar*) and bind MHC II molecules (*crescent*) on the surface of APCs (*crab shaped cells*) or astrocytes (*stretched-cornered cell*). This encounter eventually activates the transition of $CD8^+$ lymphocytes into CTL, (*spiky star*). A CTL attaches itself to an MHC class I molecule (*four-point star*) on the surface of a tumor cell, hence destroying it. The tumor cells in turn produce high levels of TGF-β (*top droplets*) reducing BBB permeability, expression of MHC II molecules and the activity of T lymphocytes. IFN-γ (*bottom droplets*) produced by CTL, increases the BBB permeability, T lymphocyte activation of MHC I and II molecules. A system of six ordinary differential equations (1–6) accounts for these dynamics

denoted C. We assume further that tumor cells that are injured by CTL are phagocytosed by APCs. In the thymus, the APC present tumor-associated antigens (TAA) that are aligned with their proper MHC antigen to naïve T cells. The maturation and proliferation of the TAA-restricted CTL proceeds in the pro-inflammatory environment. The activated T cells cross the BBB and gain access to the tumor cells. Tumor cells or Tregs, produce anti-inflammatory cytokines, such as TGF-β, that subsequently dampen the immune responses. Figure 1 is a simplified diagram of the immune responses as described in our model. A system of six ordinary differential equations (1–6) accounts for these dynamics, as described below. We use the following notation for our six-variable system: T, tumor cell number; C, total CTL number; F_β, amount of TGF-β in the tumor site; F_γ, amount of IFN-γ in the tumor; M_{I}, number of MHC class I receptors per cell; M_{II}, number of MHC class II receptors per cell.

The mathematical expressions we have chosen for representing the model conform with standards of mathematical immunology set by works such as Refs. [16, 26, 29].

Tumor dynamics

Equation (1) describes the tumor (T) dynamics,

$$\frac{\mathrm{d}T}{\mathrm{d}t} = rT\left(1-\frac{T}{K}\right) - a_T\frac{M_{\mathrm{I}}}{M_{\mathrm{I}}+e_T}\cdot\left(a_{T,\beta}+\frac{e_{T,\beta}(1-a_{T,\beta})}{F_\beta+e_{T,\beta}}\right)\cdot\frac{C\cdot T}{h_T+T}, \tag{1}$$

The first term on the right hand side (RHS) of Eq. (1) stands for tumor growth with no immune intervention, using classical logistic expression with T representing tumor cell numbers at any moment. This expression uses the concept of "carrying capacity", i.e., maximal tumor cell burden, K. The term r stands for tumor growth rate. The second term on the RHS of Eq. (1) represents tumor elimination by CTL, C, based on the assumption that it is proportional to both T and C, with saturation for large T. The saturation is represented by a linear denominator with parameter h_T standing for the accessibility of the tumor cells to CTL. The saturation factor also allows for the immunosuppressive effect of Tregs together with other known cellular immunosuppressive mechanisms. The maximal efficiency of a CTL is denoted a_T. Two other multiplicands in the elimination term introduce the effect on CTL efficiency of MHC class I receptors (M_{I}) and TGF-β (F_β) which is assumed to be a major immunosuppressive factor for CTL activity. Both effects are assumed to follow Michaelis–Menten saturation dynamics. The dependence on M_{I} is increasing from 0 to 1 with a Michaelis constant e_T. The dependence on F_β is decreasing from 1 to $a_{T,\beta}$ with Michaelis constant $e_{T,\beta}$.

CTL dynamics

CTL (C) dynamics are described by Eq. (2), below.

$$\frac{\mathrm{d}C}{\mathrm{d}t} = \left(\frac{a_{C,M_{\mathrm{II}}}M_{\mathrm{II}}\cdot T}{M_{\mathrm{II}}\cdot T+e_{C,M_{\mathrm{II}}}}\right)\cdot\left(a_{C,\beta}+\frac{e_{C,\beta}(1-a_{C,\beta})}{F_\beta+e_{C,\beta}}\right) - \mu_c\cdot C+S. \tag{2}$$

The first summand on the RHS of Eq. (2) stands for CTL recruitment from the peripheral blood system. The recruitment function [20] is positively affected by M_{II}, and the number of tumor cells, T. The dependence is implemented by Michaelis–Menten-type saturated functions. The first term increases from 0 to $a_{C,M_{\mathrm{II}}}$ with respect to

$M_{II}\cdot T$. The latter expression is the total amount of MHC class II receptors on the surface of APCs. The Michaelis parameter of this function is $e_{C,M_{II}}$. The cytokine TGF-β suppresses the proliferation and activation of T lymphocytes, as well as leukocyte migration across the BBB [17]. Therefore, the second term in the recruitment function is decreasing in F_β from 1 to $a_{C,\beta}$ with Michaelis parameter $e_{C,\beta}$. Although inflammatory reaction in the brain stimulates also Tregs to end the immune response [15, 23] for simplicity we assumed a constant death rate, μ_c for the CTL, C. The term S describes the rate of infusion of primed CTL directly to the tumor site. In the absence of immunotherapy S was set to 0.

Cytokine dynamics

Cytokine dynamics are described by Eqs. (3, 4). Equation (3) describes the dynamics of TGF-β (F_β) in the brain compartment. Equation (4) describes the dynamics of IFN-γ (F_γ).

$$\frac{dF_\beta}{dt} = g_\beta + a_{\beta,T}\cdot T - \mu_\beta \cdot F_\beta, \tag{3}$$

$$\frac{dF_\gamma}{dt} = a_{\gamma,C}\cdot C - \mu_\gamma \cdot F_\gamma, \tag{4}$$

The first term on the RHS of Eq. (3), g_β, represents the natural basal level production of bioactive TGF-β in the CNS, known to be higher than in the rest of the body [17]. The second term is the other source of TGF-β, which is the tumor [5]. We assume it to be proportional to the tumor size, $a_{\beta,T}$ being the release rate per tumor cell. The last term is the degradation of TGF-β, with constant rate, μ_β. In Eq. (4) the first term on the RHS is a linear production of IFN-γ, F_γ, where $a_{\gamma,\ C}$ is the release rate per single CTL. We assume that the only source of IFN-γ is CTL [13, 14, 19] under normal circumstances. Therefore, the amounts of IFN-γ present in the CNS are insignificant in the absence of CTL. The second term is the degradation of F_γ with constant rate, μ_γ.

MHC dynamics

MHC dynamics are described by Eqs. (5, 6). Equation (5) represents the dynamics of MHC class I (M_I) receptor molecules on a single tumor cell. Equation (6) represents the dynamics of MHC class II (M_{II}) receptor on a single APC.

$$\frac{dM_I}{dt} = g_{M_I} + \frac{a_{M_I,\gamma}\cdot F_\gamma}{F_\gamma + e_{M_I,\gamma}} - \mu_{M_I}\cdot M_I, \tag{5}$$

$$\frac{dM_{II}}{dt} = \frac{a_{M_{II},\gamma}\cdot F_\gamma}{F_\gamma + e_{M_{II},\gamma}}\cdot\left(\frac{e_{M_{II},\beta}\cdot(1-a_{M_{II},\beta})}{F_\beta + e_{M_{II},\beta}} + a_{M_{II},\beta}\right) - \mu_{M_{II}}\cdot M_{II}, \tag{6}$$

The first term on the RHS of Eq. (5) is the basal rate of M_I receptor expression per tumor cell, g_{M_I}. The second term represents the stimulation by IFN-γ of M_I expression on the surface of a GBM cell [47]. We use a Michaelis–Menten-type saturated function, where the maximal effect of IFN-γ is $a_{M_I,\gamma}$ and the Michaelis parameter is denoted $e_{M_I,\gamma}$. The last term in Eq. (5) is the degradation of M_I with constant rate, μ_{M_I}.

The first summand on the RHS of Eq. (6) represents the production rate of M_{II} per tumor cell which is a function of both IFN-γ and TGF-β. The dependence on F_γ is described by an increasing saturated function of Michaelis–Menten type with minimal value 0, maximal value $a_{M_{II},\gamma}$ and Michaelis parameter $e_{M_{II},\gamma}$. The influence of F_β is represented by a Michaelis–Menten function decreasing from 1 to $a_{M_{II},\beta}$ and Michaelis parameter $e_{M_{II},\beta}$. The second summand on the RHS of Eq. (6) is the degradation of M_{II} with constant rate, $\mu_{M_{II}}$.

Computer simulations

To use the model for retrieving potential therapeutic effects, it was implemented in the computer using a C++ code and simulated using an Euler scheme with the integration step of 0.001 h, a typical run time being a minute per simulation. The parameters had been evaluated based on published in vitro and in vivo animal and human results. The full list of references for parameter evaluation (Table 2) and the methods we applied are given in the Appendix. Two parameters, h_T and $e_{C,M_{II}}$, were estimated roughly. For the simulations of untreated tumor growth we estimated tumor cell number at the time of diagnosis and maximal tumor cell burden. Swanson et al. [41] indicate that the minimal diameter of a tumor at the time of diagnosis is 3 cm, whereas at 6 cm the patient dies. We assumed that the tumor cell density does not change during the disease progression, and that the tumor increases only in total volume, i.e., cell number. Arciero et al. [4] assume the maximal tumor cell burden to be 10^9 tumor cells per cm^3 tissue. Combining information from Arciero et al. [4] and from Swanson et al. [41] we can translate tumor size into cell numbers. Thus, a 3 cm diameter tumor at the time of diagnosis, would contain a tumor cell population of ca. 10^{10} cells. In the same manner, the tumor cells in a 6 cm diameter tumor would constitute maximal tumor cell burden of 10^{11} cells.

For the simulations of Kruse et al. trial we assumed that a residual tumor contains a number of cells comparable to the minimal detectable size. This assumption is justified even for cases where treatment followed a debulking operation on the recurrent tumor (see "Discussion"). Therefore, we used 10^{10} cells as an initial population size for these simulations as well.

Results

Retrieval of experimental results

To validate our model, we first simulated untreated grade III and GBM tumor progression. We distinguished between grade III and GBM tumors by their maximal growth rate, $r = 0.00035\ h^{-1}$ or $r = 0.001\ h^{-1}$, respectively (for details see "Appendix"). Figure 2a shows simulation results of grade III and GBM natural tumor growth, initial population sizes being two CTL and two tumor cells. Fast decline of CTL to zero ensues (not shown) and the tumor growth is uninterrupted.

Results presented in Fig. 2a are corroborated by the Burger et al. [6] estimation that a grade III tumor requires about 3–5 years to progress from the size at diagnosis to maximal size at death. Following our estimations, this correlates to growth from 10^{10} cells to 10^{11} cells (Fig. 2a, thick line). Burger et al. [6] report that GBM tumor requires about a year to progress from diagnosis size to maximal size at death, which is also in agreement with results presented in Fig. 2a (thin line).

In Fig. 2b we present the results of a simulated successful treatment for a grade III tumor arbitrarily using three infusates of 3×10^8 aCTL, infused every 5 days, followed by a 45-day interval. This treatment cycle is repeated five times over a period of 9 months (below we use the following notation to describe such a schedule: $(3 \times (3 \times 10^8$ aCTL q5d) + 45d rest) $\times$ 5). This regimen, simulating the one used by Kruse et al. [24] for grade III MG, predicts success in tumor eradication, as was, indeed, achieved in the pilot trial. We used an initial tumor population size of 10^{10} cells and small endogenous CTL initial population of 2×10^6 cells.

Next, we simulated the failure of the above regimen for GBM patients. Kruse and Rubinstein [25] report that two GBM patients died within 4 months from treatment onset. Only two aCTL infusions every 7 days per cycle were applied to these patients, and only for two cycles. We simulated this treatment, assuming a rough similarity to the untreated case, we evaluated tumor size of these GBM patients at onset to be 8×10^{10} cells. Figure 2c shows that the tumor (thick line) is hardly affected by the treatment.

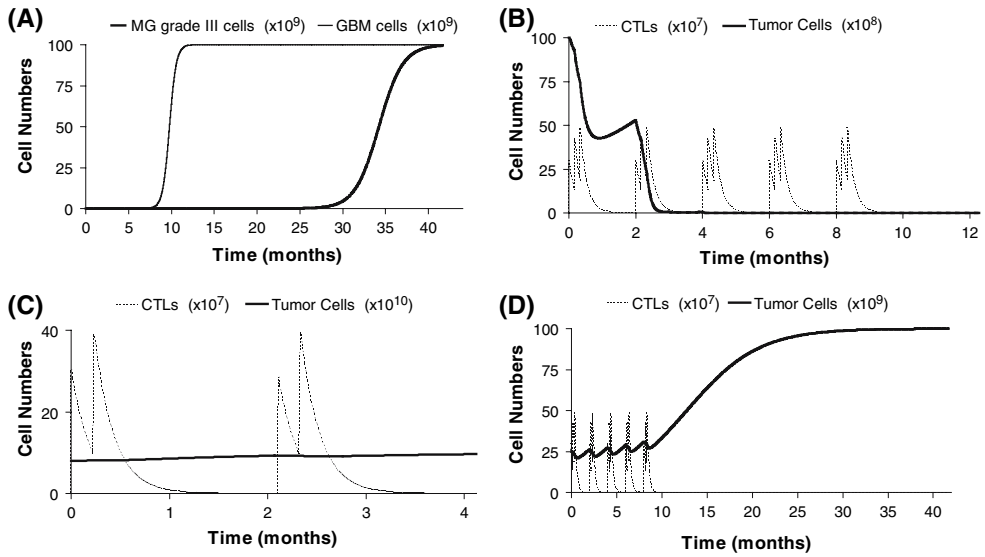

Fig. 2 Simulations retrieving experimental data. **a** Time dependent tumor growth from $T(0) = 2$, $C(0) = 2$ for grade III, $r = 0.00035\ h^{-1}$ (*thick line*), and grade IV MG, $r = 0.001\ h^{-1}$ (*thin line*). For **b**–**d** tumor cell number (*thick line*) and total CTL cell number (*dotted line*) are shown. **b** Predicted annihilation of MG Grade III by aCTL immunotherapy. aCTL immunotherapy schedule: $(3 \times (3 \times 10^8$ aCTL q5d) + 45d rest) $\times$ 5. Key parameter values were $r = 0.00035\ h^{-1}$, $T(0) = 10^{10}$, $C(0) = 2 \times 10^6$, $h_T = 5 \times 10^8$ cells. **c** Inefficient treatment of GBM (MG grade IV) by aCTL immunotherapy. aCTL immunotherapy schedule: $(2 \times (3 \times 10^8$ aCTL q7d) + 45d rest) $\times$ 2. Key parameter values were $r = 0.001\ h^{-1}$, $T(0) = 8 \times 10^{10}$, $C(0) = 2 \times 10^6$. All other parameters as in **b**. **d** Inefficient treatment of MG grade III by aCTL immunotherapy due to large initial tumor size. aCTL immunotherapy schedule: $(3 \times (3 \times 10^8$ aCTL q5d) + 45d rest) $\times$ 5. Key parameter values were $r = 0.00035\ h^{-1}$, $T(0) = 2.5 \times 10^{10}$, $C(0) = 2 \times 10^6$. All other parameters as in **b**

Model predictions

Interpretation of treatment failure

Following validation, the model was employed both for analyzing putative causes underlying the response failure of one patient in the Kruse et al. experiments, and for suggesting improved aCTL immunotherapy schedules. Simulated schedules, described below, are compared in Table 1 for their total aCTL dose and efficacy.

Kruse and Rubinstein [25] report the death of one MG grade III patient, 40 months after treatment initiation. We used our model to examine possible explanations for why the patient initially responded to treatment but later succumbed to tumor. First, we investigated the hypothesis that tumor burden of this patient at onset was considerably larger. Note that Swanson et al. [41] report a tumor size at diagnosis between 3 and 6 cm, and our above treatment simulations employed the lower estimation. We next simulated tumor growth for a tumor whose initial volume was 2.5 times larger (corresponding to a diameter of ca. 4 cm) than that simulated in Fig. 2b. As a result the applied treatment was rendered futile (Fig. 2d). Figure 2d shows that the model also reproduced Kruse and Rubinstein [25] results, namely patient's death at 40 months following treatment onset.

Another possible reason for the variable success of the MG grade III immunotherapy, is the heterogeneity of patients' tumors and their sensitivity to the innate immune system (h_T). Larger h_T values reflect reduced CTL efficiency, due to various processes. Some are hypoxia-driven, for example angiogenesis or necrosis, and are determined by surface to volume ratio. Other processes, such as Treg activation, are immunosuppressive [12]. To examine the latter possibility we simulated again the system in Fig. 2b, except that now, the tumor sensitivity is smaller, $h_T = 5 \times 10^9$. Results presented in Fig. 3a show that a larger h_T value hinders the success of aCTL immunotherapy and the tumor reaches fatal levels about 40 months after initial treatment.

An alternative cause for failure of GBM treatments, reported in Kruse et al. [24] and Kruse and Rubinstein [25] clinical trial, can be the less intensive regimen these patients received [24, 25]. To examine this possibility, we simulated treatment of GBM patients by the slightly more intensive regimens, successfully used for grade III patients (Fig. 2b). In these simulations we assumed minimal detectable tumor size at treatment onset, about 10^{10} cells. Even under this assumption, as we show in Fig. 3b, the treatment fails to eradicate the tumor, and patient's death is predicted to occur within 12 months.

Overcoming treatment failure

Due to the apparent inefficiency of immunotherapy in some grade III MG and all GBM patients we used our model to search for more efficacious immunotherapy regimens.

First, we checked the dose intensity required for eliminating refractory grade III tumors. Simulations showed that an increase in aCTL dose from 3×10^8 to 5×10^8, leaving all other regimen characteristics the same as in Fig. 2b,

Table 1 The effect of regimen on treatment success: comparison of simulation results

MG grade	T(0)	h_T	CTL dose	Inf interval (days)	Cycles	Total aCTL dose	Erad
III	10^{10}	5×10^8	3×10^8	5	5	45×10^8	Yes
IV	8×10^{10}	5×10^8	3×10^8	7	2	12×10^8	No
III	2.5×10^{10}	5×10^8	3×10^8	5	5	45×10^8	No
III	10^{10}	5×10^9	3×10^8	5	5	45×10^8	No
IV	10^{10}	5×10^8	3×10^8	5	5	45×10^8	No
III	2.5×10^{10}	5×10^8	5×10^8	5	5	75×10^8	Yes
III	2.5×10^{10}	5×10^8	3×10^8	3	5	75×10^8	Yes
III	2.5×10^{10}	5×10^8	3×10^8	4	7	84×10^8	Yes
III	10^{10}	5×10^9	2×10^9	5	5	30×10^9	Yes
III	10^{10}	5×10^9	3×10^8	1	5	22.5×10^9	Yes
III-TGF–β	10^{10}	5×10^8	2×10^8	5	5	30×10^8	Yes
III	10^{10}	5×10^8	1×10^8	2	5	35×10^8	Yes
IV	8×10^{10}	5×10^8	2×10^9	5	5	30×10^9	Yes
IV	10^{10}	5×10^8	3×10^8	4	5	60×10^8	Yes
IV	8×10^{10}	5×10^8	3×10^8	1	6	27×10^9	Yes

Inf infusion, *Erad* eradication

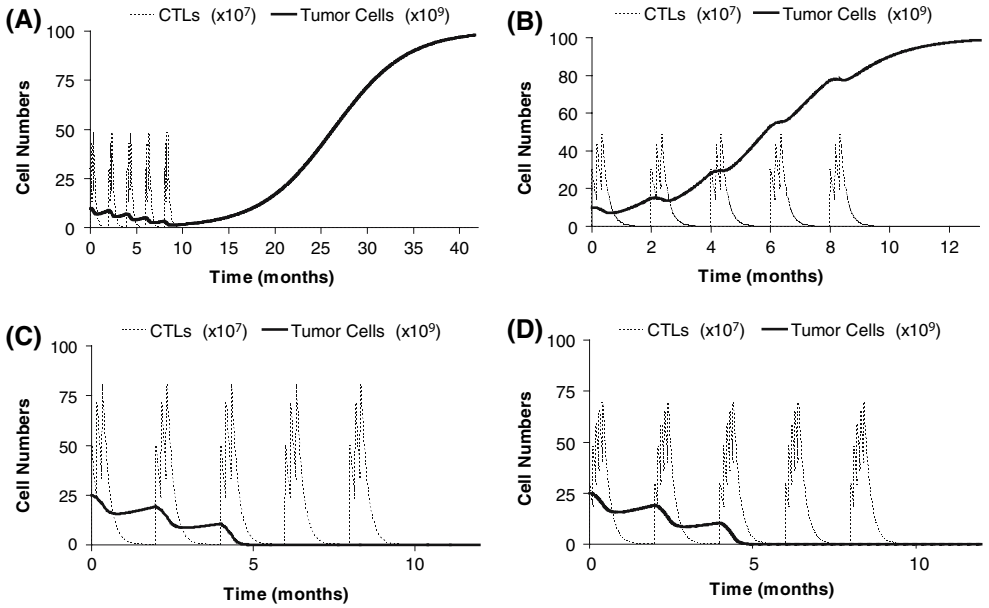

Fig. 3 Simulations of immunotherapy for MG. Tumor population (*thick line*) and total CTL level (*dotted line*) are shown. **a** Inefficient treatment of MG grade III by aCTL immunotherapy due to a large CTL-tumor efficiency parameter, h_T. aCTL immunotherapy schedule: $(3 \times (3 \times 10^8$ aCTL q5d) + 45d rest) $\times$ 5. Key parameter values were $r = 0.00035\ h^{-1}$, $h_T = 5 \times 10^9$, $T(0) = 10^{10}$, $C(0) = 2 \times 10^6$. All other parameters as in Fig. 2b. **b** Inefficient treatment of GBM using aCTL immunotherapy regimen which was effective for MG grade III. aCTL immunotherapy schedule: $(3 \times (3 \times 10^8$ aCTL q5d) + 45d rest) $\times$ 5. Key parameter values were $r = 0.001\ h^{-1}$, $T(0) = 10^{10}$, $C(0) = 2 \times 10^6$. All other parameters as in Fig. 2b. **c**, **d** Eradication of MG grade III with large initial tumor size by aCTL immunotherapy. aCTL immunotherapy schedule: **c** $(3 \times (5 \times 10^8$ aCTL q5d) + 45d rest) $\times$ 5, **d** $(5 \times (3 \times 10^8$ aCTL q5d) + 45d rest) $\times$ 5. Key parameter values were $r = 0.00035\ h^{-1}$, $T(0) = 2.5 \times 10^{10}$, $C(0) = 2 \times 10^6$. All other parameters as in Fig. 2b

provides an effective treatment for MG grade III of large initial tumor size, $T(0)$ (Fig. 3c). Alternatively, eradication of large MG grade III tumors can be achieved by increasing the infusion frequency, from once every 5 days to once every 3 days (Fig. 3d).

Further adaptations of aCTL dose intensity will yield different treatment outcomes in grade III MG with larger h_T values. Thus, in Fig. 4a we show the effect of a larger aCTL dose of 2×10^9 cells, leaving all other parameters as in the simulation shown in Fig. 2b. We compared these results to those achieved by increasing frequency of infusions to once daily. Results in Fig. 4b show that both regimens are successful in eradicating the tumor, but the total dose of aCTL in the latter regimen was 25% smaller than in the former, an important constraint on treatment feasibility. We also show (Fig. 4c) that to be efficacious, a regimen of only 80% of the aCTL dose used in the simulations presented in Fig. 2b requires infusions every 2 days.

One limitation of aCTL immunotherapy is the large numbers of aCTL needed for high dose regimens. The large numbers may concomitantly induce toxicity. Therefore, we studied methods to decrease the aCTL amounts needed. First, we examined the possibility of completely suppressing TGF-β in the system, by using TGF-β antibodies (Abs) or short inhibitory (si)RNA. To theoretically assess this approach we suppressed the model's TGF-β by setting the values of g_β and $a_{\beta,\,T}$ to 0, leaving all other parameters the same as in Fig. 2b. It can be seen in Fig. 4d that tumor eradication now requires only two-thirds of the aCTL total dose.

For examining treatment intensification strategies for GBM patients we explored many intensive treatment regimens, presenting here the ones we deemed most effective.

To eradicate small GBM tumors, i.e., 10^{10} cells at diagnosis, it suffices to use a regimen of low aCTL dose (3×10^8) at 4-day dosing-intervals (Fig. 5a). In contrast, larger GBM tumors, e.g., 8×10^{10}, will persist under a regimen of the same small aCTL dose, even when applied as frequently as once daily for five treatment cycles. However, addition of one more treatment cycle made this daily infusion regimen effective, as shown in Fig. 5b. In this case the total aCTL dose was 10% lower than in previously described high dose regimen $(3 \times (2 \times 10^9$ aCTL q5d) + 45d rest) $\times$ 5. Alternatively, we predict that large GBM tumors may be eradicated under increased aCTL dose of 2×10^9, applied every 5 days for five cycles: the same regimen as the one suggested for refractory grade III tumors (Fig. 5c).

Overall, our model predicts that a regimen of 3×10^8 cells applied every 4 days should eradicate a GBM tumor with small initial size of 10^{10} cells. Conversely, two different schedules are predicted to be as efficacious in

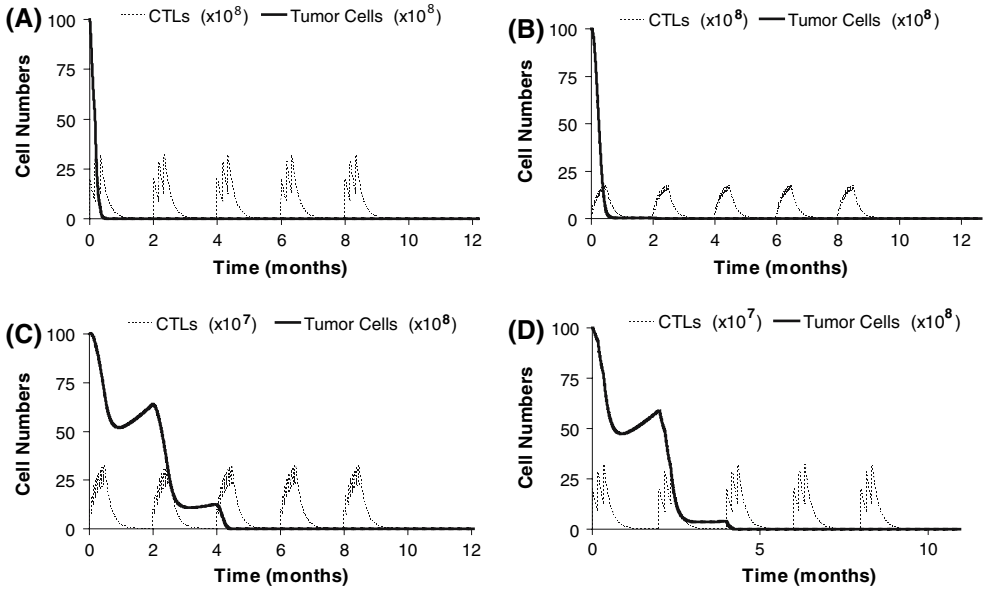

Fig. 4 Suggested immunotherapy for MG grade III. Simulation results showing tumor population (*thick line*) and total CTL level (*dotted line*) over time. **a**, **b** Eradication of MG grade III with large CTL-tumor efficiency parameter h_T by aCTL immunotherapy: **a** Large aCTL dose. aCTL immunotherapy schedule: $(3 \times (2 \times 10^9$ aCTL q5d) + 45d rest) × 5. **b** Shorter inter-dosing interval. aCTL immunotherapy schedule: $(15 \times (3 \times 10^8$ aCTL q1d) + 45d rest) × 5. Key parameter values were $r = 0.00035\ h^{-1}$, $h_T = 5 \times 10^9$, $T(0) = 10^{10}$, $C(0) = 2 \times 10^6$. All other parameters as in Fig. 2b. **c** Eradication of MG grade III by aCTL immunotherapy with an alternative regimen. aCTL immunotherapy schedule: $(7 \times (1 \times 10^8$ aCTL q2d) + 45d rest) × 5. Key parameter values were $r = 0.00035\ h^{-1}$, $T(0) = 10^{10}$, $C(0) = 2 \times 10^6$. All other parameters as in Fig. 2B. **d** Eradication of MG grade III by aCTL immunotherapy excluding the effect of TGF-β. aCTL immunotherapy schedule: $(3 \times (2 \times 10^8$ aCTL q5d) + 45d rest) × 5. Key parameter values were $g_\beta = 0$, $a_{\beta,T} = 0$, $r = 0.00035\ h^{-1}$, $T(0) = 10^{10}$, $C(0) = 2 \times 10^6$

eliminating a larger tumor of ca. 8×10^{10} cells: (1) an increased dose regimen, of 2×10^9 aCTL, applied every 5 days for five cycles; and (2) daily infusion of 3×10^8 aCTL for six cycles.

Treatment sensitivity to parameter change

An important area of exploration for developing strategies to attack this persistant tumor is to analyse which of the parameters used are the most influential on the treatment outcomes. Put in other words this analysis checks which changes in the parameters would turn, for example, a failing treatment into a successful one. From this analysis we can also learn about the treatment tolerance to errors in parameter estimation, or to patient variability. Figure 6 shows that the suggested treatment is most sensitive to the following parameters: μ_C, $T(0)$, and r. However, the treatment is tolerant to as much as 30% change in any of the model parameters, which leaves us ample margins for estimation error.

Discussion

Current MG immunotherapy research includes systemic approaches, such as virus or peptide vaccines, dendritic cells, and whole cell vaccines [27, 28, 30, 38, 43, 46]. Immunotherapy by intra-tumoral application of aCTL is less common, even though it may overcome two shortcomings of systemic MG immunotherapy, namely, the patient's anergic immune system and BBB impermeability. Nevertheless, this method has fallen out of favor in recent years, mainly due to its mixed clinical study achievements [24]. Motivated by the need to find an efficacious therapeutic method we decided to analyze these mixed results using a mathematical model whose parameters were evaluated by published experimental data (see "Appendix"). The predictions of the model concerning the life-span of patients having different MG grade tumors were confirmed by Burger et al. [6]. Notably, our predictions, relating treatment success to the patient's disease grade, were corroborated by Kruse and Rubinstein clinical trial [25]. Our predictive model will be further evaluated during a dose escalation trial, soon to be resumed. The model will be used to calculate treatment response relative to the individual tumor burden along with standardized aCTL dosages and dosing intervals.

The main conclusion of the present study is that aCTL immunotherapy is a promising therapeutic method, which may have been prematurely abandoned. Lacking better computational tools, the human treatment dosages were calculated by scaling up from pre-clinical rat experiments, regardless of tumor grade or initial tumor size [24].

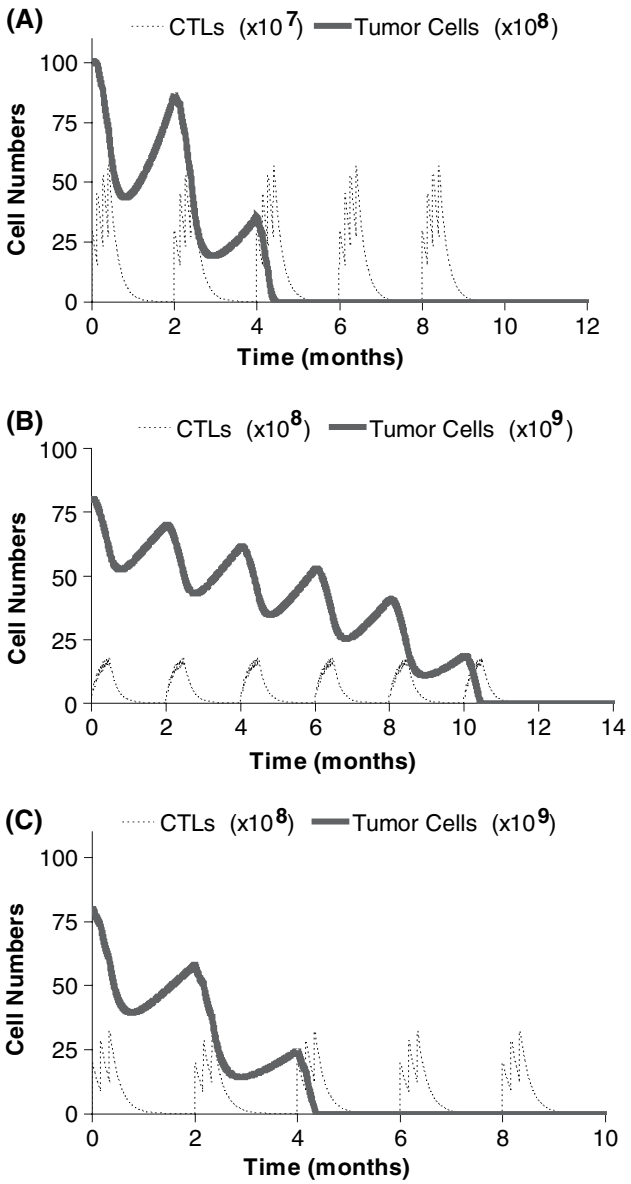

Fig. 5 Suggested immunotherapy for GBM. Simulation results showing tumor population (*thick line*) and total CTL level (*dotted line*) over time. **a** Eradication of GBM of small initial size by short inter-dose interval aCTL immunotherapy. aCTL immunotherapy schedule: $(4 \times (3 \times 10^8$ aCTL q4d) + 45d rest) × 5. Key parameter values: $r = 0.001\ h^{-1}$, $T(0) = 10^{10}$, $C(0) = 10^6$. All other parameters as in Fig. 2b. **b** Treatment of GBM of large initial size by aCTL immunotherapy at short intervals and adding one treatment cycle. aCTL immunotherapy schedule: $(15 \times (3 \times 10^8$ aCTL q1d) + 45d rest) × 6. Key parameter values were $r = 0.001\ h^{-1}$, $T(0) = 8 \times 10^{10}$, $C(0) = 6 \times 10^6$. All other parameters as in Fig. 2b. **c** Eradication of GBM of large initial size by high dose aCTL immunotherapy. aCTL immunotherapy schedule: $(3 \times (2\times 10^9$ aCTL q5d) + 45d rest) × 5. Key parameter values were $r = 0.001\ h^{-1}$, $T(0) = 8 \times 10^{10}$, $C(0) = 2 \times 10^6$. All other parameters as in Fig. 2b

Consequently, the clinically administered total aCTL dosage to GBM patients, ca. 12×10^8 aCTL, was about 20-fold smaller than that predicted by our mathematical model to be effective (27×10^9). Our results show that different grade

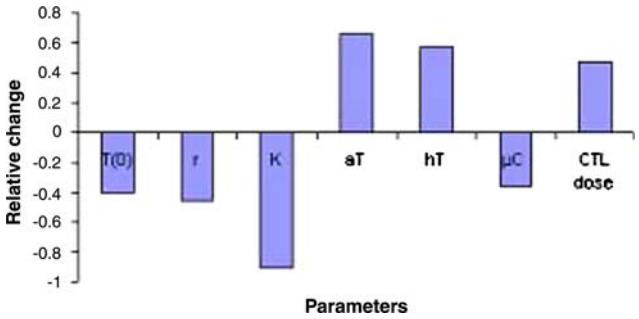

Fig. 6 Sensitivity analysis. A failed GBM treatment of small initial size $T(0) = 10^{10}$ and standard aCTL schedule $(3 \times (3 \times 10^8$ aCTL q5d) + 45d rest) × 5 becomes successful if the following parameters are changed. Each parameter was changed separately while keeping all other parameters as in Fig 2b. See appendix for parameter definitions

gliomas have different characteristic growth rates and hence warrant different, calculable, treatment intensities.

Our model suggests that the death of one MG grade III patient in Kruse's experiments 40 months after treatment initiation could be due to a larger initial tumor size, $T(0)$, or a reduced sensitivity to the immune system, h_T. The parameter h_T may be influenced by angiogenesis, Tregs, tumor surface to volume ratio, and additional factors that include the diffusive tumor growth, which may be affected differently than solid tumor growth of the same size.

The parameters r and $T(0)$ can be directly evaluated in individual patients, e.g., from imaging. The parameter h_T can be evaluated from anatomical information considering the surface to volume ratio, amount of necrosis in the tumor, proximity to blood vessels, etc. It appears, then, that our mathematical model can be an instrumental constituent of a new theranostic method for tailoring immunotherapy regimens to individual GBM patients.

Having verified (Figs. 2b–d, 3a, b) the success of the MG aCTL immunotherapy model in retrieving different clinical scenarios of Kruse et al. [24], we used it to identify improved immunotherapy schedules (Figs. 3c, d, 4a–c, 5a–c). Our model suggests that effective aCTL immunotherapy for GBM is available and that the interplay between dose, infusion frequency, and number of treatment cycles allows great flexibility in selecting the desired treatment (Fig. 5a–c). We have also shown that higher frequency of aCTL infusions can improve treatment, leading to 10–25% decrease in total aCTL dose required (Fig. 4c). However, this strategy may prove less practical due to the logistic difficulties of a 2-week period of daily infusions. To reduce CTL availability constraints we have shown that suppression of native TGF-β, by using anti TGF-β Abs or si-RNA, can reduce the CTL requirement by one-third (Fig. 4d).

An important advantage of local intra-tumoral infusion of immune cells is their mobility. Unlike common

chemotherapy or therapy by small molecules that move only by diffusion within a small radius, T cells are motile and can penetrate through large areas of the brain. Also the mode of application, using a brain canula, was designed to maximize depth of penetration and spread of T cells in tissue [Prof. Carol Kruse (Sidney Kimmel Cancer Center), personal communication]. Moreover, elimination of the major part of a tumor can make subsequent adjuvant systemic treatment (such as chemo- or radio-therapy) more effective. This concept of tumor reduction proved useful in ovarian cancer [10]. Removal of tumor mass significantly lowers the level of tumor-produced TGF-β, which, in turn, improved the host intrinsic immune response to the remaining residual cancer cells.

Overall survival of MG patients varies widely. Untreated patients survive half as long as treated patients and patients can sometimes survive with tumors larger than 6 cm in diameter, or, regretfully, die at a much smaller tumor size. Patients who participated in the Kruse et al. [24] and Kruse and Rubinstein [25] clinical trial were recurrent patients. Recurrent GBM and grade III MG patients survive only 6–9 months and 14 months, respectively [Prof. Roger Stupp (University of Lausanne Hospitals), personal communication]. This variability raises the possibility that we may have underestimated the value of maximal growth rate, r, and the maximal tumor cell burden, K. To study this possibility we have performed additional simulations with GBM growth rate values, r, corresponding to tumors at double the growth rate, and a K value ten times larger than the one used in the above-presented simulations. These simulations (not shown) were similar to the former in suggesting the same basic strategies for increasing treatment efficacy. A comprehensive study of the effect of changes in parameter values, e.g., by extension of CTL life span, on the treatment outcomes is underway.

Using aCTL in high doses should also be evaluated in light of the resultant inflammation in the CNS, a side effect caused by CTL-produced IFN-γ [45]. This side effect, along with limited availability of donor aCTL, may hinder the application of our model-suggested regimens, in cases where these involve large treatment intensification. The alternative regimens we have proposed can be used when large doses of aCTL cause an intolerable inflammatory reaction. As suggested above, the use of anti-TGF-β therapy may reduce the effective aCTL dose by up to one-third, or in cases where a larger aCTL dose will be required but unavailable. In another study, we investigate methods of circumventing the aCTL high dose requirement by increasing tumor sensitivity to aCTL as suggested by our model.

We also analyzed model sensitivity to parameters. The parameters that show the highest influence on treatment success are the death rate of aCTL, the initial size of the tumor, and its maximal growth rate. These findings hint at the direction we should follow to improve cellular immunotherapy. We can search for adjuvant treatments that would increase CTL life span. An alternative option to improve treatment success is to enhance diagnosis sensitivity and to allow for early detection. For example, the analysis shows that reducing tumor initial size by 40% would render a failed treatment successful. Yet another possible option is to reduce tumor growth rate by about one-half of its normal value, e.g., by intensive cytostatic chemotherapy. Model sensitivity analysis also suggests that the qualitative conclusions, discussed above, remain unchanged under reasonable errors in parameter estimations and inter-patient variability.

It should also be noted that the patients in the Kruse et al. trial underwent a tumor debulking operation prior to the onset of adjuvant immunotherapy. The residual tumor, remaining for the aCTL immunotherapy, taken here as the initial tumor population size, $T(0)$, could have varied, due to the unknown extent of resection for all the treated patients. Because of the diffusely infiltrative nature of the tumor cells into the healthy brain tissue, it may be undetected on an enhanced MRI scan. However, even after a gross total resection it is estimated that at least a billion tumor cells may remain. In order to allow personalized treatment, future clinical studies should accurately assess tumor burden, perhaps by tumor volumetric analyses by MRI or PET scans.

We believe that the ability of our model to predict a patient response to a suggested treatment regimen and its alterations, will aid in the development of aCTL immunotherapy. We also believe that the aCTL avenue of treatment harbors great potential, as it has already shown for grade III patients. This strategy offers bypasses to the BBB and to the patient's own weak immune system, which other immunotherapy methods are still confronting. In light of the analysis put forth in this work, we believe that further clinical trials are warranted, using mathematically calculated treatment schedules.

Acknowledgments We thank C.A. Kruse and R. Stupp for critical reading of this paper, for suggesting important corrections to the text and for contributing valuable information. We are also grateful to M. Elishmereni and to the referees for valuable revision of the manuscript. This work has been financially supported by an EU Marie Curie grant no. MRTN-CT-2004-503661 to Natalie Kronik, and by the Chai Foundation. Natalie Kronik is supported by EU Marie-Curie grant no.MRTN-CT-2004-503661. Yuri Kogan, Vladimir Vainstein, and Zvia Agur are supported by the Chai Foundation.

Appendix: Parameter estimation

In this section we present a list of all evaluated model parameters, the detailed methods and the literature sources for their evaluation (Table 2).

Table 2 Parameter estimation used in the current model

Parameter	Value	Units	Reference
r	0.00035 or 0.001	h^{-1}	Based on data from Swanson et al. [41] and Burger et al. [6]
K	1×10^{11}	cell	Arciero et al. [49]
a_T	0.12	h^{-1}	Based on data from Arciero et al. [49] and Wick et al. [60]
e_T	50	rec·cell^{-1}	Based on data from Kageyama et al. [51]
$a_{T,\beta}$	0.69	None	Thomas and Massagué [42]
$e_{T,\beta}$	10^4	pg	Based on data from Peterson et al. [55]
h_T	5×10^8 or 5×10^9	cell	Estimation fits data from Kruse et al. [24], Kruse and Rubinstein [25]
$a_{C,M_{II}}$	4.8×10^{-11}	cell·h^{-1}·rec^{-1}	Based on data from Phillips and Lampson [57] and Bosshart and Jarrett [50]
$e_{C,M_{II}}$	10^{14}	rec	Estimation
$a_{C,\beta}$	0.8	None	Based on data from Thomas and Massagué [42]
$e_{C,\beta}$	10^4	pg	Based on data from Peterson et al. [55]
μ_C	0.007	h^{-1}	Taylor et al. [58]
g_β	6.3945×10^4	pg·h^{-1}	Peterson et al. [55]
$a_{\beta,T}$	5.75×10^{-6}	pg·cell^{-1}·h^{-1}	Peterson et al. [55]
μ_β	7	h^{-1}	Coffey et al. [50]
$a_{\gamma,C}$	1.02×10^{-4}	pg·cell^{-1}·h^{-1}	Kim et al. [19]
μ_γ	0.102	h^{-1}	Turner et al. [59]
g_{M_I}	1.44	rec·cell^{-1}·h^{-1}	Based on data from Kageyama et al. [51]
$a_{M_I,\gamma}$	2.88	rec·cell^{-1}·h^{-1}	Based on data from and Yang et al. [47]
$e_{M_I,\gamma}$	3.38×10^5	pg	Based on data from Yang et al. [47], and Pharmingen manufacturer information
μ_{M_I}	0.0144	h^{-1}	Milner et al. [54]
$a_{M_{II},\gamma}$	8660	rec·cell^{-1}·h^{-1}	Based on data from Phillips et al. [56], and Bosshart and Jarrett [50]
$e_{M_{II},\gamma}$	1420	pg	Based on data from Phillips et al. [56], and Bosshart and Jarret [50]
$a_{M_{II},\beta}$	0.012	None	Based on data from Suzumura et al. [40]
$e_{M_{II},\beta}$	10^5	pg	Based on data from Suzumura et al. [40]
$\mu_{M_{II}}$	0.0144	h^{-1}	Based on data from Lazarski et al. [52]

The method for evaluating model parameters

Maximal growth rate of the tumor, r. Swanson et al. [41] assume a MG is diagnosed at 3 cm diameter and when it reaches a 6 cm diameter the patient dies. Assuming a spherical shape, the final to diagnosis initial volume ratio is $\left(\frac{6}{3}\right)^3 = 8$. We assumed that the number of tumor cells is proportional to the tumor volume. Using Eqs. (1–6), r was scaled so an untreated grade III MG (e.g., anaplastic oligodendroglioma) would grow eightfold within 3 years [6]. Thus, for grade III MG we estimated $r = 0.00035\ h^{-1}$. A GBM tumor grows from 3 cm diameter to a 6 cm diameter in about a year [41]. Using Eqs. (1–6), r was scaled to predict eightfold tumor growth within a year. Hence, for grade IV tumor we estimated $r = 0.001\ h^{-1}$.

Tumor carrying capacity (maximal tumor burden), K. Arciero et al. [4] takes the carrying capacity of tumor cells to be 10^9 cells/ml. Taking a maximal tumor diameter of 6 cm we got a volume of roughly 100 ml, which gave us an estimation of total carrying capacity of 10^{11} cells.

Maximal efficiency of CTL a_T. Wick et al. [60] report that a CTL kills 0.7–3 target cells per day. A mean value of two target cells per day gives the rate of 0.0833 cells/h. The experiment was done with 5×10^5 target cells/ml in 2 ml wells. For this calculation we used h_T value determined by Arciero et al. [4] for mice. This h_T value was smaller than the one we used later in simulations, because in vitro the contact frequency and efficacy of CTLs would be higher. Here we took h_T to be 10^5 cells/ml and multiplied it by the volume of the well. Substituting the former values into $a_T \cdot \frac{T}{h_T+T} = 0.0833\,h^{-1}$, we got $a_T = 0.12\ h^{-1}$.

Michaelis constant for the dependence of CTL efficiency on MI amount, e_T. Kageyama et al. [51] report the number of MHC I receptors per target cell to be between fewer than ten to several thousands. The value of e_T is the number of M_I receptors that brings the CTLs efficacy to half of its maximum value. Taking into account that MHC I receptors expression is suppressed in MGs, we estimated e_T to be 50 rec/cell.

Maximal reduction effect of TGF-β on CTL efficiency, $a_{T,\beta}$. Thomas and Massagué [42] report that under high concentrations of TGF-β CTL efficacy in target cell lysis has dropped to one-third after 3 h. Thus, $a_{T,\beta} = \sqrt{[3]{\frac{1}{3}}}h^{-1} \approx 0.69\,h^{-1}$.

Michaelis constant for the dependence of CTL efficiency on TGF-β amount, $e_{T,\beta}$. We took this value to be of order of magnitude of the base line found by Peterson et al. [55], multiplied by the volume of the CNS. Thus, $e_{T,\beta} = 60.9\,\mathrm{pg}\cdot\mathrm{ml}^{-1}\cdot 150\,\mathrm{ml} \approx 10^4\mathrm{pg}$.

Parameter for CTL efficiency saturation due to large tumor size, h_T. We estimated it to be $5\times\ 10^8$ cells, or 5×10^9 cells by fitting the model predictions to the the results of Kruse et al. [24], Kruse and Rubinstein [25].

Maximal effect of M_{II} on CTL recruitment, $a_{C,M_{\mathrm{II}}}$. To estimate the migration of $CD8^+$ cells across the BBB, we used Marcondes et al. [53] reporting that the number of migrating $CD4^+$ cells is similar to that of $CD8^+$ cells. According to Phillips and Lampson [57], who investigated the migration of $CD4^+$ cells, within 2 days about 40 $CD4^+$ T cells cross the BBB within a volume of a slide. We calculated the volume of a slide as its cross section area multiplied its depth: $9.2\times 10^{-6}\mathrm{m}^2\cdot 6\times 10^{-6}\mathrm{m} = 55.2\times 10^{-6}\mathrm{ml}$. Therefore, for a 100 ml tumor the maximal number of the $CD8^+$ cells recruited per hour is:

$$\frac{100\,\mathrm{ml}\cdot 40\,\mathrm{cells}}{55.2\times 10^{-6}\mathrm{ml}\cdot 48\,\mathrm{h}} \approx 1.5\times 10^6\,\mathrm{cells/h}.$$

To obtain the estimation for $a_{C,M_{\mathrm{II}}}$, we had to divide the latter number by the estimated number of MHC II receptors, which can be calculated as: (number of M II per cell) × (number of tumor cells).

Bosshart and Jarrett [49] found that the MHC II density on cell surface is about 2×10^3 rec/μm^2. We assumed half of that density (because there is poor presentation on tumor cells) and took the surface area of a cell of a diameter of 5 μm to be about 314 μm^2. For this calculation, we estimated the number of tumor cells to be 10^{11}, in agreement with the earlier assumption of 100 ml tumor volume. Thus,

$$a_{C,M_{\mathrm{II}}} = \frac{1.5\times 10^6\mathrm{cell}\cdot\mathrm{h}^{-1}}{314\,\mathrm{mm}^2\cdot\mathrm{cell}^{-1}\cdot 10^3\,\mathrm{rec}\cdot\mathrm{mm}^{-2}\cdot 10^{11}\mathrm{cells}} \approx 4.8\times 10^{-11}\,\mathrm{cell}/(\mathrm{h}\cdot\mathrm{rec}).$$

Michaelis constant for the effect of M_{II} on CTL recruitment, $e_{C,M_{\mathrm{II}}}$. We estimated that number to be 10^{14} rec. This is a rough estimation of the total number of receptors on all the tumor cells, whose number is estimated to be between 10^{10} and 10^{11} cells, while there are hundreds to thousands of receptors on each cell.

Maximal reduction effect of TGF-β on CTL recruitment, $a_{C,\beta}$. Thomas and Massagué [42] found that excess of TGF-β inhibits the proliferation of CTLs up to 50% within 3 h. Therefore, we estimated the maximal inhibition of CTL recruitment per hour by TGF-β to be $\sqrt{[3]}\frac{1}{2}\mathrm{h}^{-1} \approx 0.8\,\mathrm{h}^{-1}$.

Michaelis coefficient for the reduction effect of TGF-β on CTL recruitment, $e_{C,\beta}$. Similarly to $e_{T,\beta}$, we took this value to be of order of magnitude of the base line found by Peterson et al. [55] multiplied by the volume of the CNS. Thus, $e_{C,\beta} = 60.9\,\frac{\mathrm{pg}}{\mathrm{ml}}\cdot 150\,\mathrm{ml} \approx 10^4\mathrm{pg}$.

Death rate of CTLs, μ_C. Taylor et al. [58] find CTL half life to be 3.9 days so its hourly death rate was estimated to be $\frac{\ln 2}{72\,\mathrm{h}} \approx 0.007\,\mathrm{h}^{-1}$.

Degradation rate of TGF-β, μ_β. Coffey et al. [50] find that the hepatic half life of TGF-β is 2.2 min. Because of the distance of the liver from the and because of the necessity to pass the BBB, the actual brain TGF-β breakdown rate will be slower. We estimated it to be 6 min. Thus, the hourly breakdown rate is $\frac{\ln 2}{0.1\,\mathrm{h}^{-1}} \approx 7\,\mathrm{h}^{-1}$.

Constant base level production of TGF-β, g_β. Peterson et al. [55] found the concentration of TGF-β to be 609 pg/ml in the cerebral spinal fluid (CSF) of a GBM patient, which was tenfold higher than the level found in healthy subjects. We assumed that the volume of the CSF is 150 ml. In a healthy subject there is no tumor production of TGF-β, therefore at steady state we obtained:

$$0 = g_\beta - \mu_\beta\cdot F_\beta.$$

Thus, using previously calculated parameter values $g_\beta = 7\,\mathrm{h}^{-1}\cdot 60.9\,\frac{\mathrm{pg}}{\mathrm{ml}}\times 150\,\mathrm{ml} = 63,945\,\mathrm{pg/h}$.

Production rate of TGF-β by a single tumor cell, $a_{\beta,T}$. Using Peterson et al. [55] we found that for a GBM patient the mean level of TGF-β is $609\,\mathrm{pg}\cdot\mathrm{ml}^{-1}\cdot 150\,\mathrm{ml} = 91,350\,\mathrm{pg}$. We used previously calculated parameter values: μ_β = 7 h^{-1}, $T = 10^{11}$ cells. Using Eq. (3) at steady state, we got

$$a_{\beta,T} = \frac{91,350\,\mathrm{pg}\cdot 7\,\mathrm{h}^{-1} - 63,945\,\mathrm{pg}\cdot\mathrm{h}^{-1}}{10^{11}\,\mathrm{cells}} \approx 5.75\times 10^{-6}\,\mathrm{pg}/(\mathrm{cells}\cdot\mathrm{h}).$$

Production rate of IFN-γ by a single CTL, $a_{\gamma,C}$. Kim et al. [19] report expression of 200 pg/ml of IFN-γ by CTLs. We assumed there were $2\cdot 10^5$ CTL/ml and using μ_γ = 0.102 h^{-1} we obtained from Eq. (4) at steady state $a_{\gamma,C} = \frac{0.102\,\mathrm{h}^{-1}\cdot 200\,\mathrm{pg}\cdot\mathrm{ml}^{-1}}{2\cdot 10^5\,\mathrm{cells}\cdot\mathrm{ml}^{-1}} = 1.02\cdot 10^{-4}\,\mathrm{pg}/(\mathrm{cells}\cdot\mathrm{h})$.

Degradation rate of IFN-γ, μ_γ. Turner et al. [59] find the median half life of IFN-γ to be 6.8 h. Thus, $\mu_\gamma = \frac{\ln 2}{6.8\,\mathrm{h}} = 0.102\,\mathrm{h}^{-1}$.

Constant base level production of MHC I, $g_{M_{\mathrm{I}}}$. Kageyama et al. [51] find that the number of M_{I} receptors on cell surface varies from less than ten to several thousands. For the purpose of the following calculation we assumed M_{I} = 100 rec/cell. In the absence of IFN-γ, taking $\mu_{M_I} = 0.0144\,\mathrm{h}^{-1}$ and substituting into Eq. (5) at steady state, we obtained: $g_{M_I} = 100\,\mathrm{rec}\cdot\mathrm{cell}^{-1}\cdot\mu_{M_{\mathrm{I}}} = 1.44\,\mathrm{rec}/(\mathrm{cells}\cdot\mathrm{h})$.

Maximal production rate of MHC I induced by IFN-γ, $a_{M_{\mathrm{I}},\gamma}$. According to Yang et al. [47] the expression of MHC I receptors on some GBM tumor cells is increased threefold when subjected to excess of IFN-γ. This gave us the following ratio: $a_{M_{\mathrm{I}},\gamma} = 2 \times g_{M_{\mathrm{I}}}$, therefore $a_{M_{\mathrm{I}},\gamma} = 2.88\,\mathrm{rec/h}$.

Michaelis constant for the production rate of MHC I induced by IFN-γ,$e_{M_{\mathrm{I}},\gamma}$. Yang et al. [47] find a range of M_{I} values as a result of IFN-γ treatment. However, they display their results using a scoring scale of MHC I expression which needs to be re-scaled to receptor number. We calibrated M_{I} in the absence of IFN-γ to be equivalent to a scoring level of 1.5. Next we took the value of IFN-γ to be 100 units/ml for MHC I expression level of 2.5 according to the above score. Substituting into Eq. (5) we obtain: for $F_\gamma = 0$

$$\frac{g_{\mathrm{I}}}{\mu_{\mathrm{I}}} = 1.5,$$

and for $F_\gamma = 100$ U

$$\frac{g_{\mathrm{I}} + \frac{a_{M_{\mathrm{I}},\gamma} \cdot F_\gamma}{F_\gamma + e_{M_{\mathrm{I}},\gamma}}}{\mu_{\mathrm{I}}} = 2.5.$$

From these two equations we obtain:

$$e_{M_{\mathrm{I}},\gamma} = F_\gamma \cdot \left(\frac{3}{2}\frac{a_{M_{\mathrm{I}},\gamma}}{g_{M_{\mathrm{I}}}} - 1\right).$$

As mentioned above, the value of $\frac{a_{M_{\mathrm{I}},\gamma}}{g_{M_{\mathrm{I}}}}$ is 2. According to Pharmingen manufacturer information, the relation between the used units and IFN-γ quantities is in 0.6×10^8 units/mg. Thus, $F_\gamma = \frac{100\,\mathrm{units/ml}}{0.6 \cdot 10^8 \mathrm{units/mg}} = 1.67 \cdot 10^{-6}\,\mathrm{mg/ml}$. Substituting into the previous and taking into account the volume of 100 ml, we obtain:

$$e_{M_{\mathrm{I}},\gamma} = F_\gamma \cdot 2 \cdot 100\,\mathrm{ml} = 5 \cdot 10^{-4}\mathrm{mg} = 3.38 \cdot 10^5\,\mathrm{pg}.$$

Degradation rate of MHC I receptors, $\mu_{M_{\mathrm{I}}}$. Milner et al. [54] find that the half life of MHC I molecules varies between 6 and 96 h. We take a representative value to be 48 h. Therefore, the degradation rate is: $\frac{\ln 2}{48\,\mathrm{h}} \approx 0.0144\,\mathrm{h}^{-1}$.

Parameters for the influence of IFN-γ on MHC II expression, $a_{M_{\mathrm{II}},\gamma}, e_{M_{\mathrm{II}},\gamma}$. Phillips et al. [56] use IFN-γ injections to the brain and increase expression of MHC class II 5 fold. To scale this immunoreactivity we used data from Bosshart and Jarrett [49] who found a fourfold variation in MHC class II expression. Substituting into Eq. (6) at steady state, we obtained the following equation with two unknown variables $a_{M_{\mathrm{II}},\gamma}$ and $e_{M_{\mathrm{II}},\gamma}$:

$$\frac{a_{M_{\mathrm{II}},\gamma} \cdot F_\gamma}{F_\gamma + e_{M_{\mathrm{II}},\gamma}} - \mu_{M_{\mathrm{II}}} \cdot M_{\mathrm{II}} = 0,$$

and with two sets of parameters values:

1. $F_\gamma = 10,000\,\mathrm{U/site}$, $M_{\mathrm{II}} = 1.9 \cdot 10^3 \frac{\mathrm{rec}}{\mathrm{mm}^2} \cdot 314\,\mu\mathrm{m}^2$ ($314\,\mu\mathrm{m}^2$ being the area of cell surface) and $\mu_{M_{\mathrm{II}}} = 0.0144\,\mathrm{h}^{-1}$;
2. $F_\gamma = 30\,\mathrm{U/site}, M_{\mathrm{II}} = 0.5 \cdot 10^3 \frac{\mathrm{rec}}{\mathrm{mm}^2} \cdot 314\,\mathrm{mm}^2$ and $\mu_{M_{\mathrm{II}}} = 0.0144\,\mathrm{h}^{-1}$.

IFN-γ unit is given by 0.6×10^8 u/mg we obtained:

$$a_{M_{\mathrm{II}},g\gamma} = 8,660\,\mathrm{rec/(cells \cdot h)}..$$
$$e_{M_{\mathrm{II}},\gamma} = 1,420\,\mathrm{pg}.$$

Parameters for the influence of TGF-β on MHC II expression, $a_{M_{\mathrm{II}},\beta}, e_{M_{\mathrm{II}},\beta}$. Suzumura et al. [40] report a drop of 98.8% in MHC expression when using 100 ng/ml TGF-β. We interpreted this result as maximal inhibition and estimated: $a_{M_{\mathrm{II}},\beta} = 0.012$.

Suzumura et al. [40] report also that a dose of 10 ng/ml of TGF-β we get a drop of 89.8% in MHC expression. This gave the following equation:

$$(1 - a_{M_{\mathrm{II}},\beta})\frac{e_{M_{\mathrm{II}},\beta}}{F_b + e_{M_{\mathrm{II}},\beta}} + a_{M_{\mathrm{II}},\beta} = 0.102$$

Substituting into the above equation $F_\beta = 10\frac{\mathrm{ng}}{\mathrm{ml}} \cdot 100\,\mathrm{ml}$ we obtained:

$$e_{M_{\mathrm{II}},\beta} = 10^5\,\mathrm{pg}.$$

Degradation rate of MHC II receptors, $\mu_{M_{\mathrm{II}}}$. According to Lazarski et al. [52], MHC class II molecule half life varies between 10 and 150 h. We assumed a representing half life of 48 h and therefore $\mu_{M_{\mathrm{II}}} = \frac{\ln 2}{48\,\mathrm{h}} \approx 0.0144\,\mathrm{h}^{-1}$.

References

1. Agur Z, Arnon R, Schechter B (1988) Reduction of cytotoxicity to normal tissues by new regimes of phase-specific drugs. Math Biosci 9:1–15
2. Andaloussi AE, Lesniak MS (2006) An increase in $CD4^+$ $CD25$ $FOXP3^+$ regulatory T cells in tumor-infiltrating lymphocytes of human glioblastoma multiforme. Neurooncol 8:234–243
3. Arakelyan L, Merbl Y, Agur Z (2005) Vessel maturation effects on tumor growth: validation of a computer model in implanted human ovarian carcinoma spheroids. Eur J Cancer 41:159–167
4. Arciero JC, Jackson TL, Kirschner DE (2004) A mathematical model of tumor-immune evasion and siRNA treatment. Discret Contin Dyn S B 4:39–58
5. Bodmer S, Strommer K, Frei K, Siepl C, de Tribolet N, Heid I, Fontana A (1989) Immunosuppression and transforming growth factor-beta in glioblastoma. Preferential production of transforming growth factor-beta 2. J Immunol 143:3222–3229
6. Burger PC, Vogel FS, Green SB, Strike TA (1985) Glioblastoma multiforme and anaplastic astrocytoma, pathologic criteria and prognostic implications. Cancer 56:1106–1111
7. Cappuccio A, Elishmereni M, Agur Z (2006) Cancer immunotherapy by interleukin-21 potential treatment startegies evaluated in a mathematical model. Cancer Res 66:7293–7300

8. Carpentier PA, Begolka WS, Olson JK, Elhofy A, Karpus WJ, Miller SD (2005) Differential activation of astrocytes by innate and adaptive immune stimuli. Glia 49:360–374
9. Fine HA (2004) Toward a glioblastoma vaccine: promise and potential pitfalls. J Neurooncol 22:4240–4243
10. Goff BA, Matthews BJ, Wynn M, Muntz HG, Lishner DM, Baldwin LM (2006) Ovarian cancer: patterns of surgical care across the United States. Gyneocol Oncol 103:383–390
11. Cojocaru L, Agur Z (1992) Theoretical analysis of interval drug dosing for cell-cycle-phase-specific drugs. Math Biosci 109:85–97
12. Gomez GG, Kruse CA (2006) Mechanisms of malignant glioma immune resistence and sources of immunosupression. Gene Ther Gene Mol Biol 10:133–146
13. Gomez GG, Kruse CA (2007) Cellular and functional characterization of immunoresistant human glioma cell clones selected with alloreactive cytotoxic T lymphocytes reveals their up regulated synthesis of biologically active TGF-β. J Immunother 30:261–273
14. Gomez GG, Varella-Garcia M, Kruse CA (2006) Isolation of immunoresistant human glioma cell clones after selection with alloreactive cytotoxic T lymphocytes: cytogenetic and molecular cytogenetic characterization. Cancer Genet Cytogenet 165:121–134
15. Graf MR, Sauer JT, Merchant RE (2005) Tumor infiltration by myeloid suppressor cells in response to T cell activation in rat gliomas. J Neurooncol 73:29–36
16. Gunther N, Hoffman GW (1982) Qualitative dynamics of a network model of regulation of the immune system: a rationale for the IgM to IgG switch. J Theor Biol, pp 815–855
17. Hickey WF (2001) Basic principles of immunological surveillance of the normal central nervous system. Glia 36:118–124
18. Hussain SF, Yang D, Suki D, Aldape K, Grimm E, Heimberger AB (2006) The role of human glioma-infiltrating microglia/macrophages in mediating antitumor immune responses. Neurooncol 8:261–279
19. Kim JJ, Nottingham LK, Sin JI, Tsai A, Morrison L, Oh J, Dang K, Hu Y, Kazahaya K, Bennett M, Dentchev T, Wilson DM, Chalian AA, Boyer JD, Agadjanyan MG, Weiner DB (1998) CD8 positive T cells influence antigen-specific immune responses through the expression of chemokines. J Clin Invest 102:1112–1124
20. Kirschner D, Panetta JC (1998) Modelling immunotherapy of the tumor-immune interaction. J Math Biol 37:235–252
21. Kleihues P, Soylemazoglu F, Schäuble B, Schniethauer BW, Bruger PC (1995) Histopathology, classification, and grading of gliomas. Glia 15:211–221
22. Kleihues P, Louis DN, Scheithauer BW, Rorke LB, Reifenberger G, Burger PC, Cavenee WK (2002) The WHO classification of tumors of the nervous system. J Neuropathol Exp Neurol 61:215–225
23. Kreschmer K, Apostolou I, Jaeckel E, Khazaie K, von Boehmer H (2006) Making regulatory T cells with defined antigen specificity: role in autoimmunity and cancer. Immunol Rev 212:163–169
24. Kruse CA, Cepeda L, Owens B, Johnson SD, Stears J, Lillehei KO (1997) Treatment of recurrent glioma with intracavitary alloreactive cytotoxic T lymphocytes and Interleukin-2. Cancer Immunol Immnother 45:77–87
25. Kruse CA, Rubinstein D (2001) Cytotoxic T-lymphcytes reactive to patient major histocompatibility complex proteins for therapy of brain tumors. In: Liau LM, Becker DP, Cloughesy TF, Bigner DD (eds) Brain Tumor Immunotherapy. Humana, Totowa, pp 149–170
26. Kuznetzov VA, Makalkin IA, Taylor MA, Perelson AS (1994) Nonlinear dynamics of immunologenic tumors: parameters estimation and global bifurcation analysis. Bull Math Biol 56:295–321
27. Liau LM, Prins RM, Kiertscher SM, Odesa SK, Kremen TJ, Giovannone AJ, Lin JW, Chute DJ, Mischel PS, Cloughesy TF, Roth MD (2005) Dendritic cell vaccination in glioblastoma patients systemic and intracranial T-cell response modulated by the local central nervous system tumor microenvironment. Clin Cancer Res 11:5515–5524
28. Lopez M, Aguilera R, Perez C, Mendoza-Naranjo A, Pereda C, Ramirez M, Ferrada C, Aguillon JC, Salazar-Onfray F (2006) The role of regulatory T lymphocytes in the induced immune response mediated by biological vaccines. Immunobiology 211:127–136
29. Marchuk GI, Petrov RV, Romanyukha AA, Bocharov GA (1991) Mathematical model of antiviral immune response. I. Data analysis, generalized picture construction and parameters evaluation for hepatitis B. J Theor Biol 7–151(1):1–40
30. Morgan RA, Dudley ME, Wunderlich JR, Hughes MS, Yang JC, Sherry RM, Royal RE, Topalian SL, Kammula US, Restifo NP, Zheng Z, Nahvi A, de Vries CR, Rogers-Freezer LJ, Mavroukakis SA, Rosenberg SA (2006) Cancer regression in patients after transfer of genetically engineered lymphocytes. Science 314:126–129
31. Panek RB,Benveniste EN (1995) Class II MHC gene expression in microglia. J Immunol 154:2846–2854
32. de Pillis LG, Radunskaya AE, Wiseman CL (2005) A validated mathematical model of cell-mediated immune response to tumor growth. Cancer Res 65:7950–7958
33. de Pillis LG, Gu W, Radunskaya AE (2006) Mixed immunotherapy and chemotherapy of tumors: modeling, applications and biological interpretations. J Theor Biol 238:841–862
34. Proescholdt MA, Merrill MJ, Ikejiri B, Walbridge S, Akbasak A, Jacobson S, Oldfield EH (2001) Site-specific immune response to implanted gliomas. J Neurosurg 95:1012–1019
35. Read SB, Kulprathipanja NV, Gomez GG, Paul DB, Winston KR, Robbins JM, Kruse CA (2003) Human alloreactive CTL interactions with gliomas and with those having upregulated HLA expression from exogenous IFN-γ or IFN-γ gene modification. J Interferon Cytokine Res 23:379–393
36. Skomorovski K, Harpak H, Ianovski A, Vardi M, Visser TP, Hartong SC, van Vliet HH, Wagemaker G, Agur Z (2003) New TPO treatment schedules of increased safety and efficacy: pre clinical validation of a thrombopoiesis simulation model. Br J Haematol 123:683–691
37. Soos JM, Krieger JI, Stuve O, King CL, Patarroyo JC, Aldape K, Wosik K, Slavin AJ, Nelson PA, Antel JP, Zamvil SS (2001) Malignant glioma cells use MHC class II transactivator (CIITA) promoters III and IV to direct IFN-γ-inducible CIITA expression and can function as nonprofessional antigen presenting cells in endocytic processing and CD4+ T-cell activation. Glia 36:391–405
38. Steiner HH, Bonsanto MM, Beckhove P, Brysch M, Geletneky K, Ahmadi R, Schuele-Freyer R, Kremer P, Ranaie G, Matejic D, Bauer H, Kiessling M, Kunze S, Schirrmacher V, Herold-Mende C (2004) Antitumor vaccination of patients with glioblastoma multiforme: a pilot study to assess feasibility, safety, and clinical benefit. J Clin Oncol 22:4272–4281
39. Strik HM, Stoll M, Meyermann R (2004) Immune cell infiltration of intrinsic and metastatic intracranial tumors. Anticancer Res 24:37–42
40. Suzumura A, Sawada M, Yamamoto H, Marunouchi T (1993) Transforming growth factor-β suppresses activation and proliferation of microglia in vitro. J Immunol 151:2150–2158
41. Swanson KR, Bridge C, Murray JD, Alvord EC Jr (2003) Virtual and real brain tumors: using mathematical modeling to quantify glioma growth and invasion. J Neurol Sci 216:1–10

42. Thomas DA and Massagué J (2005) TGF-β directly targets cytotoxic T cell functions during tumor evasion of immune surveillance. Cancer Cell 8:369–380
43. de Vleeschouwer S, Rapp M, Sorg R, Steiger H, van Gool S, Sabel M (2006) Dendritic cell vaccination in patients with malignant gliomas: current status and future directions. Neurosurgery 59:988–999
44. Weller M, Fontana A (1995) The failure of current immunotherapy for malignant glioma. Tumor-derived TGF-beta, T-cell apoptosis, and the immune privilege of the brain. Brain Res Brain Res Rev 21:128–151
45. Wheeler RD, Zehntner SP, Kelly LM, Bourbonniere L, Owens T (2006) Elevated interferon gamma expression in the central nervous system of tumor necrosis factor receptor 1-deficient mice with experimental autoimmune encephalomyelitis. Immunology 118:527–538
46. Wiseman CL, Kharazi A (2006) Objective clinical regression of metastatic breast cancer in disparate sites after use of whole cell vaccine genetically modified to release Sargarmostim. Breast J 12:475–480
47. Yang I, Kremen TJ, Giovannone AJ, Paik E, Odesa SK, Prins RM, Liau LM (2004) Modulation of major histocompatibility-complex class I molecules and major histocompatibility complex-bound immunogenic peptides induced by interferon α and interferonγ treatment of human glioblastoma multiforme. J Neurosurg 100:310–319
48. Zagzag D, Salnikow K, Chiriboga L, Yee H, Lan L, Ali MA, Garcia R, Demaria S, Newcomb EW (2005) Downregulation of major histocompatibility complex antigens in invading glioma cells: stealth invasion of the brain. Lab Invest 85:328–341
49. Bosshart H and Jarrett RF (1998) Deficient major histocopatibility complex class II antigen presentation in a subset of Hodgkin's disease tumor cells. Blood 92:2252–2259
50. Coffey RJ, Kost LJ, Lyons RM, Moses HL, LaRusso NF (1987) Hepatic processing of transforming growth factor β in the rat uptake, metabolism, and biliary excretion. J Clin Invest 80:750–757
51. Kageyama S, Tsomides TJ, Sykulev Y, Eisen HN (1995) Variations in the number of peptide–MHC class I complexes required to activate cytotoxic T cell responses. J Immunol 154:567–576
52. Lazarski CA, Chaves FA, Jenks SA, Wu S, Richards KA, Weaver JM, Sant AJ (2005) The Kinetic stability of MHC class II: peptide complexes is a key parameter that dictates immunodominance. Immunity 23:29–40
53. Marcondes MC, Burudi EM, Huitron-Resendiz S, Sanchez-Alavez M, Watry D, Zandonatti M, Henriksen SJ, Fox HS (2001) Highly activated $CD8^+$T cells in the brain correlate with early central nervous system dysfunction in simian immunodeficiency virus infection. J Immunol 167:5421–5438
54. Milner E, Barnea E, Beer I, Admon A (2006) The turnover kinetics of MHC peptides of human cancer cells. Mol Cell Proteomics 5:366–378
55. Peterson PK, Chao CC, Hu S, Thielen K, Shaskan E (1992) Glioblastoma, transforming growth factor-β, and *Candida* meningitis: a potential link. Am J Med 92:262–264
56. Phillips LM, Simon PJ, Lampson LA (1999) Site-specific immune regulation in the brain: differential modulation of major histocompatibility complex (MHC) proteins in brainstem vs. hippocampus. J Comp Neurol 405:322–333
57. Phillips LM, Lampson LA (1999) Site-specific control of T cell traffic in the brain: T cell entry to brainstem vs. hippocampus after local injection of IFN-γ. J Neuroimmunol 96:218–227
58. Taylor GP, Hall SE, Navarrete S, Michie CA, Davis R, Witkover AD, Rossor M, Nowak MA, Rudge P, Matutes E, Bangham CR, Weber JN (1999) Effect of Lamivudine on human T-cell leukemia virus type 1 (HTLV-1) DNA copy number, T-cell phenotype, and anti-tax cytotoxic T-cell frequency in patients with HTLV-1-associated myelopathy. J Virol 73:10289–10295
59. Turner PK, Houghton JA, Petak I, Tillman DM, Douglas L, Schwartzberg L, Billups CA, Panetta JC, Stewart CF (2004) Interferon-gamma pharmacokinetics and pharmacodynamics in patients with colorectal cancer. Cancer Chemother Pharmacol 53:253–260
60. Wick WD, Yang OO, Corey L, Self SG (2005) How many human immunodeficiency virus type 1-infecfted target cells can a cytotoxic T-lymphocyte kill? J Virol 79:13579–13586